

Development of Short-Wavelength Far-Infrared Lasers and Optical Elements for Plasma Diagnostics

Kazuya NAKAYAMA, Masahiro TOMIMOTO, Shigeki OKAJIMA, Kazuo KAWAHATA¹⁾, Kenji TANAKA¹⁾, Tokihiko TOKUZAWA¹⁾, Tsuyoshi AKIYAMA¹⁾ and Yasuhiko ITO¹⁾

Chubu University, Kasugai, Aichi 487-8501, Japan

¹⁾*National Institute for Fusion Science, Toki, Gifu 509-5259, Japan*

(Received 10 December 2006 / Accepted 11 March 2007)

Powerful 48- and 57- μm CH_3OD lasers pumped by a 9R(8) CO_2 laser have been developed to establish a new two-color FIR laser interferometer system for high density and large volume plasma diagnostics. To design the collimated beams for the interferometer, the beam profiles and the divergence angles have been measured for the 48- and 57- μm CH_3OD lasers oscillated simultaneously. Water vapor absorptions for the laser wavelengths have been measured at 22 °C to realize an efficient transmission line. Optical constants and transmittance and reflectance of crystal quartz, silicon, CVD-diamond, polyethylene sheet, Mylar film, TPX plate, metal mesh and wire grid have been measured to design the optical components (observation windows and beam splitters) in the 48- and 57- μm laser interferometer system.

© 2007 The Japan Society of Plasma Science and Nuclear Fusion Research

Keywords: far-infrared (FIR) laser, water vapor absorption of FIR laser beam, refractive index and absorption coefficient for FIR region, FIR laser interferometer, plasma diagnostics

DOI: 10.1585/pfr.2.S1114

1. Introduction

Far-infrared (FIR) lasers have been utilized as optical sources to measure an electron density of fusion plasmas. In the Large Helical Device (LHD) at National Institute for Fusion Science (NIFS), the electron density profile has been measured by a 13-channel Michelson interferometer using a cw 119- μm CH_3OH laser, routinely [1]. For a high density operation of the LHD and future plasma devices such as the International Thermonuclear Experimental Reactor (ITER), short-wavelength FIR lasers in the region of 40 to 70 μm are superior to the 119- μm CH_3OH laser and a 10- μm CO_2 laser from viewpoints of the plasma refraction and mechanical vibration effects and the fringe shifts in the interferometer [2]. For the purpose, powerfully and simultaneously oscillated 48- and 57- μm CH_3OD lasers which pumped by a cw 9R(8) CO_2 laser have been developed [3]. By Kawahata *et al.*, a new two-color interferometer using these CH_3OD lasers has been proposed [4]. To establish the laser interferometer system, the beam profiles and the divergence angles have been measured for the CH_3OD lasers. In the FIR region, water vapor absorption of the laser beam is one of several problems for beam transmission. To realize the efficient transmission line, water vapor absorptions for the laser wavelengths have been measured. To design the optical components (observation windows and beam splitters) in the laser interferometer system, optical constants and transmittance (reflectance) for the interest materials (crystal quartz, silicon, CVD-diamond, etc.) have been measured. In this paper, those results will be re-

ported.

2. Development of 50- μm Lasers

Although many FIR lasers have been reported [5], usable and powerful short wavelength FIR lasers of 40 to 70 μm region have not been well known. Using an FIR laser system pumped by a cw CO_2 laser as shown in Fig. 1, we have searched powerful FIR lasers from CH_3OH and the isotopes for the wavelength region. The FIR laser is twin type, and the cavity length is about 2.9 m. The laser tube is of 25-mm-inner-diameter with a water-jacket made by Pyrex glass. The laser cavity is constructed with two flat coupling mirrors. The input coupler has a 3 mm-diameter off-axis hole to prevent feedback effect of the

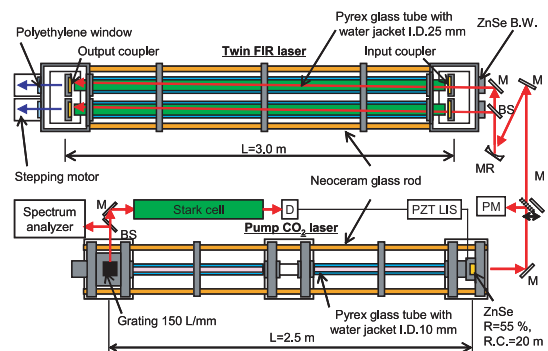


Fig. 1 A schematic drawing of the CO_2 laser pumped twin FIR laser system.

author's e-mail: nakayama@isc.chubu.ac.jp

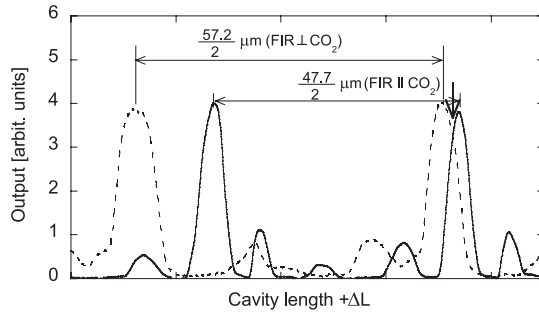


Fig. 2 Detuning curves of 48- μm (—) and 57- μm (----) lasers.

CO_2 laser beam for pumping. The output coupler is silicon hybrid mirror with a 8-mm-diameter clear aperture at its center.

We have discovered the most powerful 48- and 57- μm CH_3OD lasers pumped by a 9R(8) CO_2 laser [3]. The polarization of the 48- μm laser is parallel to that of the pump CO_2 laser, while that of the 57- μm laser is perpendicular. Both lasers oscillate simultaneously at every 143 μm of the cavity length ($57.1511/2 \mu\text{m} \times 5 = 142.878 \mu\text{m}$ and $47.65/2 \mu\text{m} \times 6 = 143.0 \mu\text{m}$) as shown in Fig. 2, and are useful for the sources of the two-color FIR laser interferometer.

3. Propagation Properties of 50- μm Lasers

To design collimated beams for the two-color laser interferometer with these lasers, the intensity profiles at the distances of 1.2, 2.2, and 3.3 m from the output coupler have been measured. As shown in Fig. 3, the intensity distribution of the beam was confirmed to be Gaussian, but the cross section of the beam was ellipse form slightly. This is caused by a bending of the laser tube. The beam radius ω which the beam intensity falls to $1/e^2$ of each peak value at those points were calculated and shown in Fig. 4. The beam divergences θ ($\theta = \lambda/\pi\omega_0$) which calculated as the beam waist ω_0 is 2.5 mm for 48- and 57- μm lasers are estimated to be 6.1×10^{-3} and 7.3×10^{-3} rad., respectively. Although there is a difference in the divergence angle, it is possible to apply the interferometer with a long distance transmission by a proper choice of concave and convex mirrors.

In the FIR region, water vapor absorption in the atmosphere is one of severe problems for beam transmission. Although water vapor absorption for some FIR laser wavelengths has been reported [6–8], the reliable values for the 48- and 57- μm in wavelength have not been reported yet. Accordingly, we have measured those for 48-, 57-, and 119- μm laser lines by using the measurement system shown in Fig. 5. The absorption cell is a 1.25-m-long glass tube with an inner diameter of 90 mm, and the both ends are shielded by a 1 mm-thick polyethylene sheets. The humidity in the cell was adjusted by a moist air and a dry

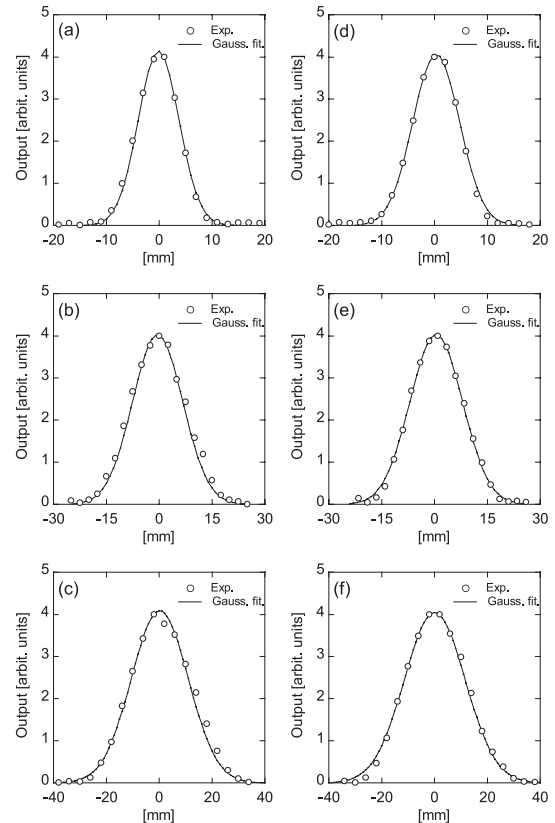


Fig. 3 Beam profiles of (a)-(c) 48- μm and (d)-(f) 57- μm lasers. Graphs (a) and (d) are at the distance of 1.2 m from the output coupler. Graphs (b) and (e) are at the distance of 2.2 m. Graphs (c) and (f) are at the distance of 3.3 m.

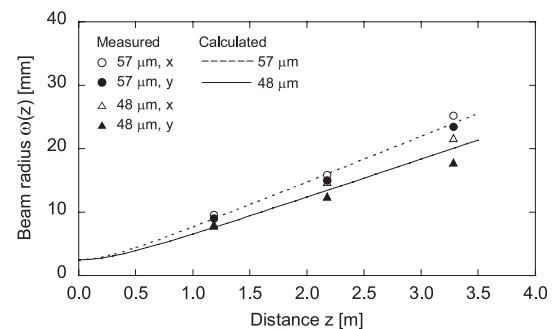


Fig. 4 Beam propagations of 48- and 57- μm lasers. z is the distance from the output mirror.

air. The humidity and temperature were measured by two thermometer/hygrometer at inner both ends. The transmitted laser power after passing through the absorption cell was detected by a pyroelectric detector, and the transmissivity was calculated by using the monitored reference signal, and normalized to 1.0 at 0% in humidity in a vacuum. The results which were carried out at 22°C are shown in Fig. 6. The transmissivity decreases linearly with increasing the humidity within about 40%. The absorption coefficients at vapor density of 7.5 g/m^3 estimated by the report of Gallagher *et al.*, [6] for 119 μm (84.2 cm^{-1}), 57.2 μm

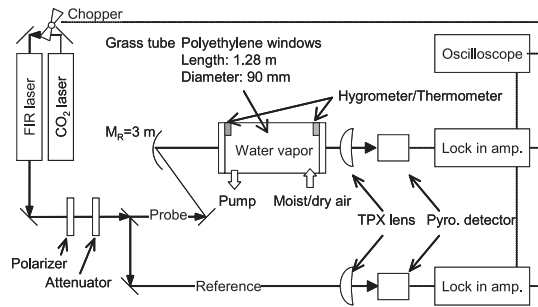


Fig. 5 A block diagram of the measurement of water vapor absorption.

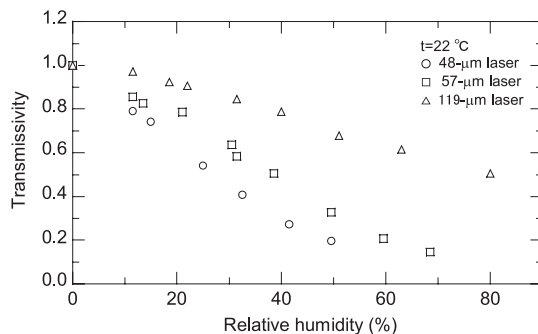


Fig. 6 Transmissivity of water vapor in the atmosphere as a function of relative humidity for 48-, 57-, and 119- μm lasers.

(175 cm^{-1}), and $47.6\text{ }\mu\text{m}$ (210 cm^{-1}) are about 0.18 m^{-1} , 0.46 m^{-1} , and 0.46 m^{-1} , respectively. In our experiments, the vapor density corresponds to the humidity of 39%, and the coefficients are 0.19 m^{-1} for the 119- μm , 0.57 m^{-1} for the 57- μm and 0.91 m^{-1} for the 48- μm . Although the measured coefficient for the 119- μm line was in agreement with the estimated value, those values for the 48- and 57- μm lines were larger. If the 48- and 57- μm lasers are transmitted for a distance of 10 m in the air of $22\text{ }^{\circ}\text{C}$ and 10%, the attenuations are 84% for 48 μm and 70% for 57 μm . It is therefore very important to eliminate humidity when the 48- and 57- μm lasers were used in the interferometer system.

4. Optical Elements for 50- μm Interferometer System

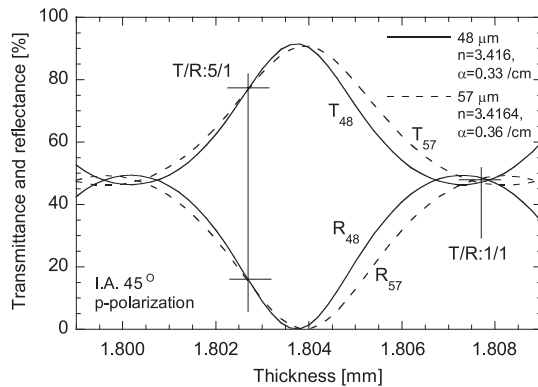
A selection of an optimal optical material of optical elements (observation windows and beam splitters) is important in order to construct the interferometer using the 48- and 57- μm lasers. Requirements of optical materials are as follows: small absorption, high strength and low outgas for a high vacuum, high rigidity for a microphonic vibration, and so on. For the two-color measurement system, optical materials which can be together used for these lasers are required. In order to design the efficient optical elements, it is necessary to know precise optical con-

stants. Although the refractive index and absorption coefficient of crystal quartz and silicon measured by Fourier spectrometry have been reported [9–11], the reliable optical constants measured by these laser wavelengths have not been reported, yet. Therefore we have measured refractive index and absorption coefficient of a crystal quartz etalon, a silicon etalon with high resistivity ($2.8\text{ k}\Omega\text{cm}$), and a CVD diamond etalon [12] and transmittance and reflectance of a polyethylene seat, a TPX plate, a Mylar film, a metal mesh, and a free standing wire grid. The optical constants have been obtained from the transmission measurement of a rotating etalon [12]. In this measurement, the accuracy of refractive index depends strongly on that of the etalon's thickness and the laser wavelength. The thicknesses of samples are $1.5845 \pm 0.0002\text{ mm}$ for the crystal quartz etalon, $2.1704 \pm 0.0003\text{ mm}$, $2.1718 \pm 0.0003\text{ mm}$, and $1.5452 \pm 0.0003\text{ mm}$ for the silicon etalon, and $1.023 \pm 0.001\text{ mm}$ for the CVD diamond etalon.

Table 1 shows the measurement results of optical constants of crystal quartz, CVD-diamond, and silicon. The measured values of crystal quartz are agreement with the values measured by Fourier spectrometry [9]. The optical constants values obtained by Russell *et al.*, [9] at 175 cm^{-1} ($57.2\text{ }\mu\text{m}$) are $n_o = 2.1760 \pm 0.001$, $n_e = 2.2310 \pm 0.001$, $\alpha_o = 3.8 \pm 0.4\text{ cm}^{-1}$, and $\alpha_e = 2.7 \pm 0.3\text{ cm}^{-1}$. Our results of silicon are different from the values measured by Fourier spectrometry [11]. The optical constants values of silicon ($100\text{ }\Omega\text{cm}$) obtained by Loewenstein *et al.*, [11] at 175 cm^{-1} ($57.2\text{ }\mu\text{m}$) are $n = 3.4195 \pm 0.002$ and $\alpha = 1.2 \pm 0.3\text{ cm}^{-1}$. The difference in the optical constants is believed to be due to the different resistivity and temperature [10]. Table 2 shows the transmittance and reflectance of polyethylene, TPX, Mylar, metal mesh, and wire grid at 45° incidence. The transmittance and reflectance of each material are indicated the values of p-polarization at the 57- μm laser and that of s-polarization at the 48- μm laser. Owing to the large absorption, it is very difficult to use crystal quartz and Mylar. Polyethylene sheets can be used as a laser window. Metal mesh and wire grid is small absorption, and it is possible to obtain an optional transmissivity and reflectivity by changing the wire width and space. However, the type is limited by the diffraction effect. The absorption coefficient of CVD-diamond is smaller than other materials expect for metal mesh and wire grid. The CVD-diamond etalon is excellent material as observation windows and beam splitters from view points of the properties (small absorption, high strength, and transparency in visible light). Because the interferometer is composed of many beam splitters, the silicon etalon with low absorption is useful material, also. Although silicon is not transparency in visible light, a YAG laser ($\lambda = 1.06\text{ }\mu\text{m}$) makes possible alignment of the interferometer. Shown in Fig. 7 are the data from example design of a common beam splitter using a silicon etalon for the 48- and 57- μm lasers. Consequently, for proposed new two color interferometer, it was made sure that designing

Table 1 Optical constants of crystal quartz, CVD-diamond, and silicon for 48- and 57- μm laser lines.

| Sample | 57.1511 μm | | 47.65 μm | |
|--|-----------------------|-----------------|---------------------|-----------------|
| | n | α [/cm] | n | α [/cm] |
| Crystal quartz (ordinary ray) | 2.1764 \pm 0.0002 | 3.8 \pm 0.1 | 2.219 \pm 0.001 | 6.4 \pm 0.2 |
| Crystal quartz (extraordinary ray) | 2.2306 \pm 0.0002 | 2.9 \pm 0.1 | 2.260 \pm 0.001 | 4.9 \pm 0.2 |
| CVD-diamond | 2.383 \pm 0.002 | 0.19 \pm 0.05 | 2.383 \pm 0.002 | 0.33 \pm 0.05 |
| Silicon (2.8 k Ωcm , 20 $^{\circ}\text{C}$) | 3.4164 \pm 0.0005 | 0.36 \pm 0.05 | 3.416 \pm 0.001 | 0.25 \pm 0.05 |

Fig. 7 Example design of silicon beam splitters for 48- and 57- μm lasers.Table 2 Transmittance and reflectance of polyethylene, TPX, Mylar, metal mesh, and wire grid at 45 $^{\circ}$ incidence for 48- and 57- μm lasers.

| Sample | 57.1511 μm | | 47.65 μm | |
|----------------------------------|-----------------------|--------|---------------------|--------|
| | Tp [%] | Rp [%] | Ts [%] | Rs [%] |
| Polyethylene (h=0.9 mm) | 85 | 1 | 70 | 6 |
| TPX (h=3.06 mm) | 66 | 2 | 47 | 10 |
| Mylar film (h=0.05 mm) | 64 | 4 | 51 | 14 |
| Metal mesh (#1000) ¹⁾ | 29 | 68 | 23 | 74 |
| Wire grid ²⁾ | 93 | 2 | 89 | 6 |

1) Wire width 7.4 μm , hole size 18 μm 2) Wire diameter 5 μm , wire spacing 12.5 μm

The electric field of the laser is perpendicular to the wire.

of beam splitters and windows with optimal transmittance and reflectance was possible by a choice of the etalon's thickness.

5. Conclusions

In the present work beam divergence angles, water vapor absorption, and optical constants of some materials have been measured to establish a two color interferometer using 48- and 57- μm CH₃OD lasers oscillated simultaneously. Intensity distributions have been measured at distances $z = 1.2, 2.2$, and 3.3 m from the laser output mirror. The beam divergence angles for the 48- laser and 57- μm lasers have been found to be 6.1×10^{-3} rad and 7.3×10^{-3} rad, respectively. Water vapor absorptions in the

air of the 48- and 57- μm lasers are larger than that of a 119- μm CH₃OH laser. The absorption coefficients at 39 % in relative humidity (22 $^{\circ}\text{C}$) have been obtained 0.19 m^{-1} for the 119- μm laser, 0.57 m^{-1} for the 57- μm laser and 0.91 m^{-1} for the 48- μm laser. This result indicates that a complete dehumidification is necessary for a long distance transmission. We confirmed that beam propagations of the 48- and 57- μm lasers could be designed for the interferometer of a long distance. Optical constants of some materials (crystal quartz, silicon, and CVD-diamond etalons and a polyethylene sheet, a Mylar film, a TPX plate, a metal mesh, and a wire grid) have been measured to use as observation windows and beam splitters for the 48- and 57- μm lasers. As a result, it has been found that a CVD-diamond and high resistive silicon etalons are useful material. It is possible to design common-use windows and beam splitters for these lasers by using our measurements results. Therefore, we recommend the 48- and 57- μm lasers as optical sources, CVD-diamond etalons as the observation window, and silicon etalons as the beam splitters, for the 50- μm two color laser interferometer system for plasma with high density and large volume.

Acknowledgments

This study was supported by a grant from the High-Tech Research Center Establishment Project (Chubu University) and a Grants-in-Aid for Scientific Research (NIFS) from Ministry of Education, Culture, Sports, Science and Technology.

- [1] K. Kawahata *et al.*, Rev. Sci. Instrum. **70**, 707 (1999).
- [2] S. Okajima *et al.*, Rev. Sci. Instrum. **72**, 1094 (2001).
- [3] K. Nakayama *et al.*, Rev. Sci. Instrum. **75**, 329 (2004).
- [4] K. Kawahata *et al.*, Rev. Sci. Instrum. **75**, 3508 (2004).
- [5] M.J. Weber, *Hand Book of Laser Wavelengths* (CRC Press, 1999).
- [6] J.J. Gallagher *et al.*, Infrared Physics **17**, 43 (1977).
- [7] D.E. Evans *et al.*, Opt. Commun. **22**, 337 (1977).
- [8] O.A. Simpson *et al.*, J. Phys. Chem. **84**, 1753 (1980).
- [9] E.E. Russell *et al.*, J. Opt. Soc. Am. **57**, 342 (1967).
- [10] M.N. Afsar *et al.*, Infrared Phys. **18**, 835 (1978).
- [11] E.V. Loewenstein *et al.*, Applied Optics **12**, 398 (1973).
- [12] K. Nakayama *et al.*, Int. J. Infrared Millim. Waves **24**, 1421 (2003).
- [13] D.A. Naylor *et al.*, Applied Optics **17**, 1055 (1978).